Research Article

Journal of PeptideScience

Received: 28 September 2010 Revised: 15 October 2010 Accepted: 25 October 2010 Published online in Wiley Online Library: 4 February 2011

(wileyonlinelibrary.com) DOI 10.1002/psc.1333

Neuroglobin–prion protein interaction: what's the function?‡

Pasquale Palladino,[a] Giovanni Luca Scaglione,[b] Alessandro Arcovito,[b] Rosa Maria Vitale,[c] Pietro Amodeo,[c] Beatrice Vallone,[d] Maurizio Brunori,[d] Ettore Benedetti[a] and Filomena Rossi[a]*

Neuroglobin and cellular prion protein (PrP^C) are expressed in the nervous system and co-localized in the retinal ganglion cell layer. Both proteins do not have an unambiguously assigned function, and it was recently reported that PrP^C aggregates rapidly in the presence of neuroglobin, whereas it does not aggregate in the presence of myoglobin, another globin with different tissue specificity. Electrostatic complementarity between the unstructured PrP^C *N*-terminus and neuroglobin has been proposed to mediate this specific interaction. To verifythis hypothesis experimentally, we have used a combined approach of automated docking and molecular dynamics (MD) studies carried out on short stretches of prion protein (PrP) *N*-terminus to identify the minimal electrostatically interacting aminoacidic sequences with neuroglobin. Subsequently, we have performed the synthesis of these peptides by solid phase methods, and we tested their interaction with neuroglobin by surface plasmon resonance (SPR). Preliminary results confirm unequivocally the specific interaction between synthetic PrP peptides and neuroglobin suggesting a crucial role of PrP^C positively charged regions in thisprotein–protein association. Copyright © 2011 European Peptide Society and John Wiley & Sons, Ltd.

Keywords: neuroglobin; cellular prion protein; peptides synthesis; surface plasmon resonance; nervous system

Introduction

Several disorders, such as Alzheimer's, Parkinson's and prion diseases, are classified as conformational diseases because they are related to misfolding which leads to the intracellular accumulation of protein aggregates. In particular, misfolding of prion protein (PrP) is related to transmissible spongiform encephalopathy (TSE) [1].

PrP is a glycoprotein, mainly expressed in the nervous system, with a large number of partners covering all cell compartments in which PrP amount depends on organs, cell-type and PrP mutations. In detail, typical extracellular PrP shows its *C*-terminal globular domain anchored by glycosylphosphatidylinositol (GPI) to the cell surface, even if in some neurons it is confined mainly to the cytosol. Moreover, in the brain, some amount of PrP is found in endoplasmatic reticulum (ER) membrane, with the unstructured *N*-terminus domain exposed to the cytosol and the *C*-terminus inside the ER lumen, or *vice versa*, because the PrP hydrophobic region limits the complete translocation of PrP [2]. As prion accumulation in the cytosol is the key event associated with neurotoxicity, it is important to better characterize the interaction of PrP with its intracellular partners to decipher the role of naturally occurring cellular prion protein (PrP^C) [3].

Recently, neuroglobin (Ngb) was identified as a new member of cytosolic PrP interactome [4]. Ngb reversibly binds O_2, can act as a NO scavenger and is predominantly observed in the cytosol of neurons and retina [5–7]. Ngb shows the typical globin fold, but it has low sequence similarity with vertebrate myoglobin and hemoglobin; moreover, the hexacoordination of iron with two endogenous histidines in the absence of external ligands and the unusual sliding of the heme into a preformed cavity upon CO binding are peculiar properties of this protein [8].

It was reported that PrP and Ngb are co-localized in the retinal ganglion cell layer. PrP aggregates rapidly in the presence of Ngb, without prion misfolding, whereas it does not aggregate in the presence of myoglobin, thus suggesting electrostatic complementarity between the unstructured PrP *N*-terminus and Ngb, with a specific role of neuroglobin as scavenger of cytosolic prion molecules [4].

Here we report a study on short stretches of PrP *N*-terminus identified as potential electrostatically interacting regions of Ngb by a combined approach of automated docking and molecular dynamics (MD) studies. These peptides were synthesized by solid phase methods and their interaction with Ngb was tested by surface plasmon resonance (SPR) technique. Our data assign the interaction between PrP *N*-terminus region and Ngb to a specific

* *Correspondence to: Filomena Rossi, Dipartimento delle Scienze Biologiche & CIRPeB, Università degli Studi di Napoli "Federico II", IT-80134 Napoli, Italy. E-mail: filomena.rossi@unina.it*

a *Dipartimento delle Scienze Biologiche & CIRPeB, Università degli Studi di Napoli "Federico II", IT-80134 Napoli, Italy*

b *Istituto di Biochimica e Biochimica Clinica, Università Cattolica del Sacro Cuore di Roma, IT-00168 Roma, Italy*

c *Istituto di Chimica Biomolecolare (ICB)-CNR, IT-80078 Pozzuoli, Italy*

d *Dipartimento di Scienze Biochimiche, Università degli Studi di Roma "La Sapienza", IT-00185 Roma, Italy*

‡ *Special issue devoted to contributions presented at "Peptides at work: From Structure to Applications", 12th Naples Workshop on Bioactive Peptides and 2nd Italy-Korea Symposium on Antimicrobial Peptides, 4-7 June 2010.*

sequence motif, confirming a crucial role of PrP positively charged regions in protein–protein association.

Materials and Methods

Chemicals

All solvents were reagent grade. *Nα*-Fmoc-protected amino acids and activating agents were purchased from Inbios (Pozzuoli, Italy). Resin for peptides synthesis was from Novabiochem (Läufelfingen, Switzerland). HPLC chemicals were purchased from Lab-Scan (Dublin, Ireland). Columns for peptide purification and characterization were from Phenomenex (Torrance, CA, USA).

Peptide Synthesis

The PrP derived peptides *C*-terminal protected by amide (Am) group corresponding to the sequences: KKRPKPGGWNTGGSRYPGQGS, PrP[23–43]Am; KKRPKPGGW, PrP[23–31]Am; and full protected *N*-acetylated (Ac) and *C*-amidated form of the prion *N*-terminus: NTGGSRYPGQGS PrP[32–43]AcAm, were synthesized in batch by standard 9-Fmoc chemistry protocol using Rink-amide 4-methylbenzhydrylamine (MBHA) resin. Amino acids coupling was achieved using *N*-HOBt: *O*-benzotriazole-*N*,*N*,*N*′,*N*′-tetramethyl-uronium-hexafluoro-phosphate (HBTU): *N*,*N*-DIEA (1 : 1 : 1v/v/v) for 10 min. Fmoc removal was achieved by 30% piperidine/DMF treatment for 10 min. Acetylation was carried out by 1 M acetic anhydride in DMF containing 5% DIEA. Peptide deprotection and cleavage from the solid support was achieved by treatment with a TFA/triisopropylsilane (TIS)/water (95 : 2.5 : 2.5, v/v/v) mixture for 120 min at room temperature. The crude peptides were precipitated at 0 °C with ethyl ether, dissolved in a water/acetonitrile (1 : 1, v/v) mixture, and lyophilized. Products were purified by RP-HPLC using a C_{18} Jupiter (250 Å; 22 mm) column applying a linear gradient of acetonitrile/0.1% TFA in water/0.1% TFA from 5 to 70% over 30 min (flow rate: 20 ml/min). Peptide purity and integrity were confirmed by LC–MS (Finnigan Surveyor, Thermo Electron Corporation). Characterization was conducted under standard conditions of peptide analysis. The expected and experimental mass of peptides are: PrP[23–43]Am (2214.5 Da; 1108.4 *m/z* $[M + 2H]^{2+}$); PrP[23–31]Am (1052.3 Da; 1054.3 *m/z* $[M + H]^{+}$); PrP[32–43]AcAm; (1221.2 Da; 1221.7 $[M + H]^{+}$).

Surface Plasmon Resonance

Nitrilotriacetate (NTA) group is activated by nickel ions (Ni^{2+}) to bind selectively histidine-tagged neuroglobin, which can be stripped from the surface by removing the nickel ions with ethylenediaminetetraacetic acid (EDTA) or other chemicals (regeneration phase). The sensor chip surface is reconstructed with fresh histidine-tagged protein in every cycle of the assay. SPR assay was performed at 25 °C and at flow rate of 30 µl/min; association phase was followed for 180s, while dissociation phase was followed for 300 s with PrP peptide fragments. Analytes were dissolved in NTA running buffer, 10 mM *N*′-2-hydroxyethylpiperazine-*N*′-2-ethanesulphonic acid (Hepes) 150 mM NaCl 50 µM EDTA and 0.005% (v/v) P20 (non-ionic surfactant) at pH 7.4. To regenerate chip, complete dissociation of complexes formed were achieved by addition of 10 mM Hepes, 150 mM NaCl, 350 mM EDTA, 0.005% (v/v) P20, pH 8.3 for 30 s before each new cycle start. Dissociation constants (K_D) were estimated by Scatchard plot analysis using the Biacore X100 evaluation software.

Molecular Dynamics

Amidated prion peptides 23–28, 23–31 and 23–43, built with the leap module of Amber9 package, were sampled and refined with a restrained simulated annealing (SA) protocol, using the Sander classic module of AMBER6 [9] with AMBER all-atom 1994 parametrization [10], followed by energy minimization with the Sander module of AMBER9 [11], parm99 [12] force field and the GB^{HCT}/SA methodology [13] to represent solvation effects. A full-extended structure underwent 50 SA cycles of 100 000 MD steps, where system temperature was linearly raised from 10 to 1200 K (steps 1–5000), then kept constant at 1200 K (steps 5001–50 000), and finally, linearly decreased down to 10 K (steps 50 001–100 000). A time step of 1 fs, with no constraints or restraints on bond lengths, a non-bonded cutoff of 16 Å and a 0.05 fs time constant for heat bath coupling were used, with all other parameters set at their default values. All peptide bonds were forced into a *trans* conformation ($\omega = 180^{\circ}$) by torsional constraints with a force constant of 50 kcal mol^{-1} operating for deviations higher than 20° from *trans* form. Chirality restraints were also applied to ensure proper amino acid chiralities and prochiralities. Final structures were energy minimized (EM) with 100 steps of steepest descent followed by a conjugate gradient method, down to a gradient norm value less than 10^{-3} kcal mol^{-1} $Å^{-1}$. Cluster analysis of resulting conformers was done with MOLMOL program [14].

Docking studies were performed with version 4.0 of AutoDock [15]. The crystallographic structure of murine Ngb (PDB entry 1Q1F) [16] and 23–28 prion peptide were treated with AutoDock tools (ADT) package [17] to merge non-polar hydrogens, calculate Gasteiger charges and desolvation parameters and select side chain peptide bonds allowed to rotate. Grids for docking evaluation were generated using the program AutoGrid 4.0 included in AutoDock 4.0 distribution. Three grid boxes of $80 \times 72 \times 80$ points with a spacing of 0.375 and different grid center values were calculated around the protein to explore its entire surface. Lamarckian genetic algorithm (LGA) was adopted to perform molecular docking. The docking parameters employed were the following: 50 individuals in a population with a maximum of 15 million energy evaluations and a maximum of 37 000 generations, followed by 300 iterations of Solis and Wets local search. A total of 50 docking runs were performed for each calculation. The peptide was allowed to flexibly dock with its side chains, but the protein remained rigid during docking. Each docking gave an ensemble of ligand docking modes: the structure with most favorable binding energy was selected for the subsequent MD simulation of peptide–Ngb complex.

To perform MD simulation in solvent, minimized peptide 23–43 alone and peptide 23–28 in complex with Ngb were confined in truncated octahedron boxes ($x, y, z = 50$ and 80 Å, respectively) filled with TIP3P water molecules and counterions (Na^{+}) to neutralize the system. The solvated molecules were then EM through 1000 steps with solute atoms restrained to their starting positions using a force constant of 10 kcal mol^{-1} $Å^{-1}$ before MD simulations. After this, the molecules were submitted to 90 ps restrained MD (5 kcal mol^{-1} $Å^{-1}$) at constant volume, gradually heating to 300 K, followed by 60 ps restrained MD (5 kcal mol^{-1} $Å^{-1}$) at constant pressure to adjust system density. To preserve sodium ion coordination geometry distance restraints of 30 kcal mol^{-1} $Å^{-1}$ between the sodium ion and all atoms involved in ion binding were applied during energy minimization and MD equilibration. Production MD simulations were carried

Journal of PeptideScience

out at 300 K and a constant pressure for 3 ns with a time step of 1.5 fs. Bonds involving hydrogens were constrained using the SHAKE algorithm [18].

Results and Discussion

Models for Ngb–PrP peptide complex have been obtained by flexible docking followed by MD simulations, starting from the hypothesis of electrostatic interaction between PrP *N*-terminus region and Ngb. However, even for a relatively small peptide, full-flexible docking would result in a too limited exploration of relative protein/peptide orientations. In fact, the total sampled configuration space results from the multiplication of the number of relative protein/peptide orientations by that of peptide internal degrees of freedom. So, in order to substantially restrict the explored subspace of PrP peptide internal degrees of freedom, we used SA to identify starting conformations for PrP peptide backbone, to be used subsequently in flexible docking calculations, where flexibility was only retained for PrP peptide side chains. PrP peptide used for docking studies encompasses residues 23–28 of PrP protein, i.e. the motif KKRPKP, selected on the basis of the high number of consecutive charged residues and because of the presence of two proline residues able to restrain the conformational space accessible to this peptide. Fifty conformers, obtained by an SA protocol described in 'Materials and Methods', were clusterized with the 'CalcCluster' command of MOLMOL program, using min and max root mean square deviation (RMSD) values of 0.05 and 1.5 Å, respectively, after backbone superimposition for residues from 24 to 28. Cluster analysis produced 12 clusters, consisting of 8, 3, 20, 1, 4, 1, 2, 4, 3, 2, 2 conformers, respectively. The MOLMOL 'representative' structure from the most populated cluster (RMSD value for 24–28 residues is 0.528 Å) was used for the subsequent docking calculations. Both the most populated cluster and most of the minor ones, with the exception of 9 of 50 conformers, were all characterized by mostly to fully extended conformations, devoid of any stabilizing non-sequential interactions, as confirmed by CD analysis (data not shown). In this view, the representative conformer from the main cluster is also representative of conformations occurring in about 80% of annealing structures, also taking into account the large rearrangements that such extended conformations can undergo during long, fully unrestrained MD simulations, such as those used in the refinement of our final complex (see below). To explore the entire neuroglobin protein surface, the docking was carried out using a multi-step approach, in which overlapping regions of protein were explored separately, in order to achieve a higher spatial resolution for a given total number of energy evaluations in comparison with a single docking step employing a unique grid encompassing the full protein volume. The complex with most favorable binding energy out of the resulting 100 ones obtained from autodock runs, shown in Figure 1, was then subjected to fully unrestrained MD simulations of 6 ns, to assess its stability. The analysis of MD trajectory revealed a quite stable complex, in which the peptide is located in a narrow cleft lined by both acidic (Glu51, Asp52 and Glu58), and polar residues (Asn43, Ser48, Ser55 and Gln46). To facilitate experimental studies of such PrP peptide–Ngb interactions, the peptide was elongated by three residues, thus including a Trp residue, useful for further study of fluorescence. An SA on PrP[23–31] peptide showed that the backbone conformation of 23–28 residues in the most populated cluster does not appreciably differ from that observed in the annealing of

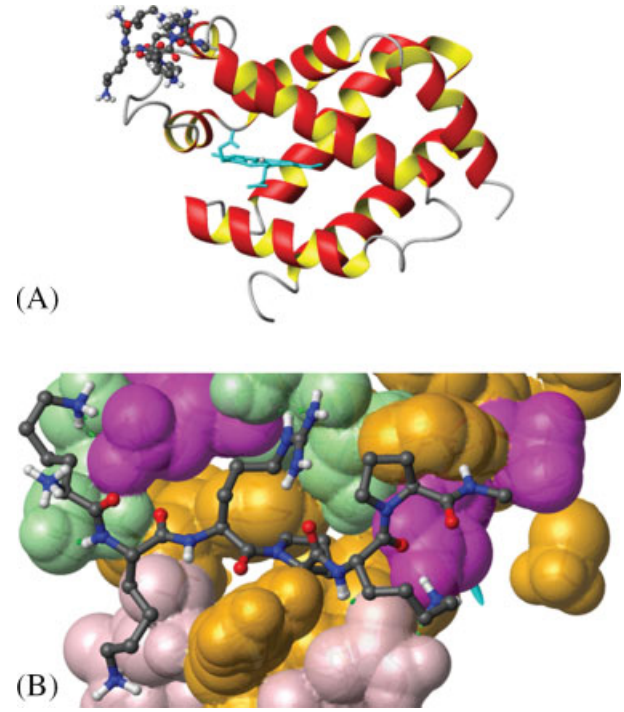

Figure 1. (A) Best model of Ngb protein–PrP peptide complex. Protein is depicted as red–yellow ribbon for helices and gray tube for other regions, while cyan sticks are used for heme prosthetic group. Peptide is shown in a ball-and-stick representation colored according atom types. (B) Detail of the Ngb protein–PrP peptide binding region. A semi-transparent surface plus sticks is used for protein, colored orange for generic, magenta for acidic Asp and Glu, pink for Asn and Gln, light-green for Thr and Ser residues. Peptide is shown in a ball-and-stick representation colored according atom types. Intermolecular H-bonds and salt-bridges are depicted as green dotted sticks.

PrP[23–28]. Moreover, we decided to synthesize a longer version of this peptide, PrP[23–43], to include also polar residues that could, in principle, improve interaction with the target protein. Nevertheless, as detailed below, SPR assay of prion derived peptide binding to Ngb showed for fragment PrP[23–43]Am a dissociation constant slightly higher than PrP[23–31]Am. As PrP[32–43]AcAm is not able to bind Ngb, it is possible that this region somehow reduces the ability of prion *N*-terminus 23–31 to interact with Ngb. To verify this hypothesis, PrP[23–43]Am was subjected to SA and for the most stable conformation a 3 ns MD simulation in solutions was carried out. While PrP[23–28] is characterized by a mostly extended conformation, lacking any non-sequential interaction, the longer peptide PrP[23–43] exhibits for most of the simulated time partly bent conformations, stabilized by interactions involving polar and positively charged side chains (data not shown). Such intramolecular interactions could compete with the intermolecular ones, unfavorably affecting the positively charged stretch recognition by Ngb. The lack of any detectable interaction of Ngb with PrP[32–43]AcAm strongly suggests that the recognition PrP–Ngb is mainly electrostatic.

In Table 1 the sequence of PrP *N*-terminus derived peptides is given, namely PrP[23–31]Am, PrP[23–43]Am and PrP[32–43]AcAm. The interaction between PrP peptides (analytes) with purified His-tagged Ngb (ligand) was measured by SPR technique, using Biacore X100 instrument (Biacore, Uppsala, Sweden). PrP peptides association with Ngb was tested in a concentration range from 10 μM to 156 nM and the measured dissociation

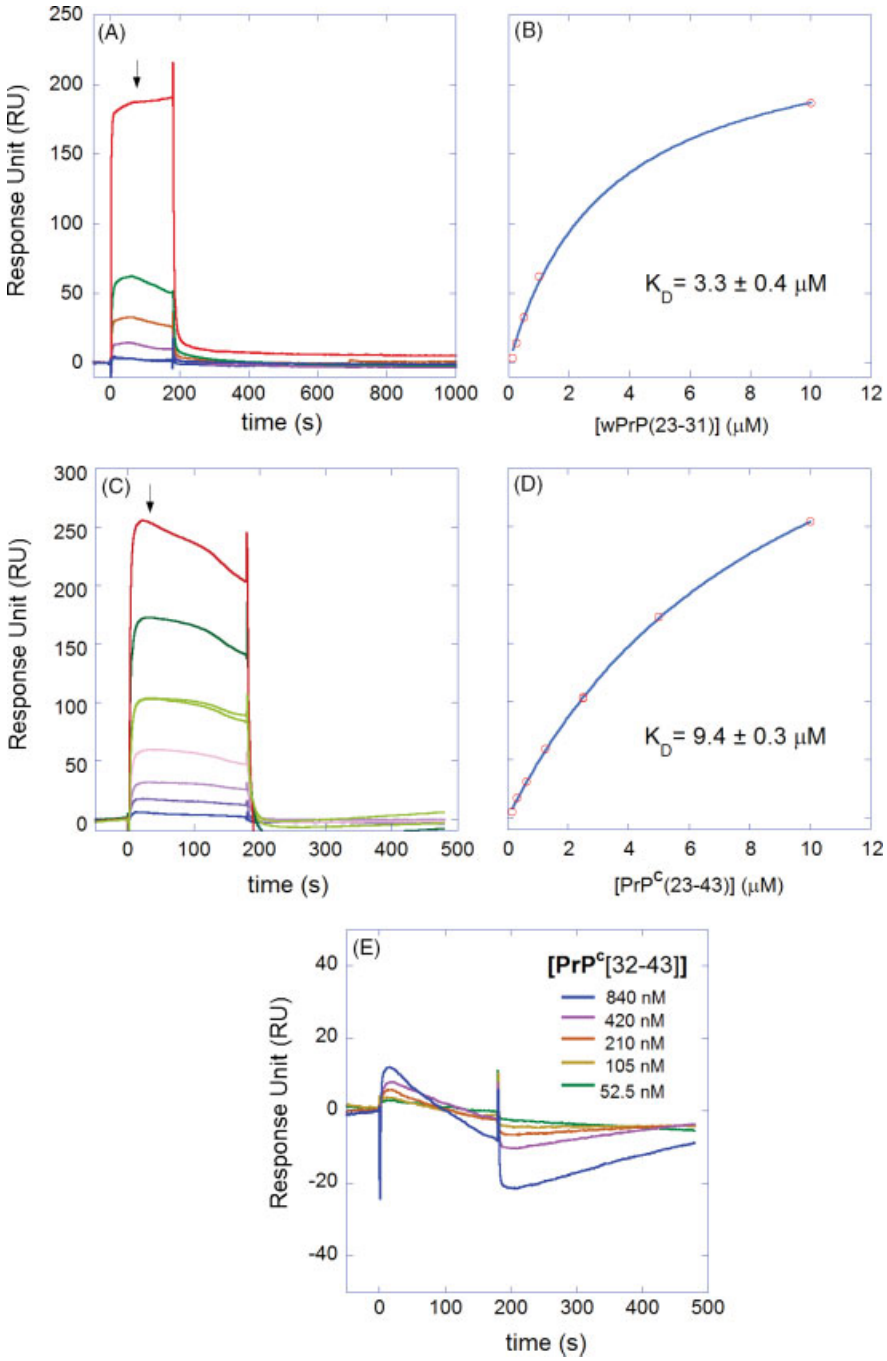

Figure 2. SPR assay of prion peptide fragments binding to Neuroglobin. Neuroglobin was bound to an NTA chip as described in Materials and Methods and used as a ligand. The injection of different analytes was in the concentration range from 10 μM to 156 nM. (A) and (B) The sensorgrams and the Scatchard plot of the prion peptide PrP[23–31]. (C) and (D) The corresponding pictures of the prion peptide PrP[23–43]Am. The arrow indicates the time after the injection that has been used to calculate the response of the instrument to determine the Scatchard plot. (E) The sensorgrams for the prion peptide PrP[32–43] that show no interaction with the Ngb protein in the concentration range investigated.

constants are reported in Table 1. In Figure 2 the sensorgrams and the corresponding Scatchard plots, when available, are displayed.

The strongest direct interaction was observed between Ngb and the shortest peptide PrP[23–31]Am, with a dissociation constant $K_D = 3.3 \pm 0.4\,\mu M$. Consistently with the simulations carried out by means of MD, the value observed for the longer peptide still containing the *N*-terminal sequence, PrP[23–43]Am, yielded a value of $K_D = 9.4 \pm 0.3\,\mu M$ that accounts for a slightly decreased affinity. Peptide PrP[32–43]AcAm, showed no

Table 1. Biacore SPR assay of PrP peptides binding to Ngb

Analyte	Sequence	K_D (10^{-6} M)
PrP[23–31]Am	KKRPKPGGW-Am	3.3 ± 0.4
PrP[23–43]Am	KKRPKPGGWNTGGSR YPGQGS-Am	9.4 ± 0.3
PrP[32–43]AcAm	Ac-NTGGSRYPGQGS-Am	Not detected

Journal of PeptideScience

interaction confirming that binding is specific for the sequence corresponding to PrP[23–31] and it is not due to association with generic peptides of a given length. Therefore these experiments, carried out at physiological ionic strength (150 mM NaCl), indicate that, although the interaction PrP[23–31]–Ngb is electrostatic, it is still able to mediate association between PrP and Ngb. Thus, future experiments will be performed as a function of ionic strength to better characterize this recognition mechanism. However, binding via the positively charged processed *N*-terminus PrP (after maturation by proteolytic cleavage before Lys23) has been previously reported for tubulin [19] and microtubule associated proteins (MAPs, i.e. Tau [20–22]). The interaction of PrP with tubulin is among the best characterized and has been assigned to peptide PrP[23–33], with an association constant comparable with the one observed for Ngb (0.88 μM). Thus, in the retina where Ngb is abundant (about 100 μM), it can interfere with PrP association with other cytoplasmic proteins, including tubulin. This hypothesis could account for resistance of retinal ganglion cells to scrapie PrP inoculation and formation of PrP^C cytosolic aggregates without cell death [5]. Therefore, sequestering of PrP^C by Ngb could counteract the adverse effects due to interference of PrP^C with several cytoplasmic proteins [4]. Indeed, many other PrP interacting proteins are described in the cell, but there are few data on their quantitative binding to PrP^C; remarkably the measured association constants, when available, are in the same range of what we have observed for the interaction between PrP peptides and Ngb [4,23–25]. Our data provide quantitative evidence of the molecular interaction between Ngb and PrP *N*-terminus derived peptide, and could contribute to the identification of new molecules to devise TSE therapy with a notable interest for conformational diseases responsible of many ocular disorders [25].

Acknowledgements

The authors acknowledge the 'Internazionalizzazione del Sistema Universitario 2004-2006', MIUR D.M. 5.8.2004 n.262, art. 26, for its support to this research and MIUR grants 20074TJ3ZB 005 and RBRN07BMCT 007.

References

1 Prusiner SB. Prions. *Proc. Natl. Acad. Sci. U.S.A.* 1998; **95**: 13363–13368.
2 Stewart RS, Harris DA. Mutational analysis of topological determinants in prion protein (PrP) and measurement of transmembrane and cytosolic PrP during prion infection. *J. Biol. Chem.* 2003; **278**: 45960–45968.
3 Nieznanski K. Interactions of prion protein with intracellular proteins: so many partners and no consequences? *Cell. Mol. Neurobiol.* 2010; **30**: 653–656.
4 Lechauve C, Rezaei H, Celier C, Kiger L, Corral-Debrinski M, Noinville S, Chauvierre C, Hamdane D, Pato C, Marden MC. Neuroglobin and prion cellular localization: investigation of a potential interaction. *J. Mol. Biol.* 2009; **388**: 968–977.
5 Giuffrè A, Moschetti T, Vallone B, Brunori M. Is neuroglobin a signal transducer? *IUBMB Life* 2008; **60**: 410–413.
6 Brunori M, Giuffrè A, Nienhaus K, Nienhaus GU, Scandurra FM, Vallone B. Neuroglobin, nitric oxide, and oxygen: functional pathways and conformational changes. *Proc. Natl. Acad. Sci. U.S.A.* 2005; **102**: 8483–8488.
7 Vallone B, Nienhaus K, Matthes A, Brunori M, Nienhaus GU. The structure of carbonmonoxy neuroglobin reveals a heme-sliding mechanism for control of ligand affinity. *Proc. Natl. Acad. Sci. U.S.A.* 2004; **101**: 17351–17356.
8 Burmester T, Hankeln T. What is the function of neuroglobin? *J. Exp. Biol.* 2009; **212**: 1423–1428.
9 Simmerling CL, Darden TA, Merz KM, Stanton RV, Cheng AL, Vincent JJ, Crowley M, Tsui V, Radmer R, Duan Y, Pitera J, Massova I, Seibel GL, Singh UC, Weiner PK, Kollman PA. *AMBER 6*. University of California: San Francisco, 1999.
10 Cornell WD, Cieplak P, Bayly CI, Gould IR, Merz KM Jr, Ferguson DM, Spellmeyer DC, Fox T, Caldwell JW, Kollman PA. A second generation force field for the simulation of proteins, nucleic acids, and organic molecules. *J. Am. Chem. Soc.* 1995; **117**: 5179–5197.
11 Case DA, Darden TA, Cheatham TE III, Simmerling CL, Wang J, Duke RE, Luo R, Merz KM, Pearlman DA, Crowley M, Walker RC, Zhang W, Wang B, Hayik S, Roitberg A, Seabra G, Wong KF, Paesani F, Wu X, Brozell S, Tsui V, Gohlke H, Yang L, Tan C, Mongan J, Hornak V, Cui G, Beroza P, Mathews DH, Schafmeister C, Ross WS, Kollman PA. *AMBER 9*. University of California: San Francisco, 2006.
12 Wang J, Cieplak P, Kollman PA. How well does a restrained electrostatic potential (RESP) model perform in calculating conformational energies of organic and biological molecules? *J. Comput. Chem.* 2000; **21**: 1049–1074.
13 Tsui V, Case DA. Theory and applications of the generalized born solvation model in macromolecular simulations. *Biopolymers (Nucl. Acid. Sci.)* 2001; **56**: 275–291.
14 Koradi R, Billeter M, Wüthrich K. MOLMOL: a program for display and analysis of macromolecular structures. *J. Mol. Graph.* 1996; **14**: 51–55.
15 Morris GM, Goodsell DS, Halliday RS, Huey R, Hart WE, Belew RK, Olson AJ. Automated docking using a Lamarckian genetic algorithm and an empirical binding free energy function. *J. Comput. Chem.* 1998; **19**: 1639–1662.
16 Vallone B, Nienhaus K, Brunori M, Nienhaus GU. The structure of murine neuroglobin: novel pathways for ligand migration and binding. *Proteins* 2004; **56**: 85–92.
17 Sanner MF. Python: a programming language for software integration and development. *J. Mol. Graph. Model.* 1999; **17**: 57–61.
18 Ryckaert J-P, Ciccotti G, Berendsen HJC. Numerical integration of the cartesian equations of motion of a system with constraints: molecular dynamics of *n*-alkanes. *J. Comput. Phys.* 1977; **23**: 327–341.
19 Osiecka KM, Nieznanska H, Skowronek KJ, Karolczak J, Schneider G, Nieznanski K. Prion protein region 23–32 interacts with tubulin and inhibits microtubule assembly. *Proteins* 2009; **77**: 279–296.
20 Han J, Wang X, Yao H, Gao C, Li F, Zhang B, Jiang H, Dong X. Tau-mediated microtubule formation inhibited by prion protein. *Neurosci. Bull.* 2005; **21**: 398–403.
21 Han J, Zhang J, Yao H, Wang X, Li F, Chen L, Gao C, Gao J, Nie K, Zhou W, Dong X. Study on interaction between microtubule associated protein tau and prion protein. *Sci. China C. Life Sci.* 2006; **49**: 473–479.
22 Wang XF, Dong CF, Zhang J, Wan YZ, Li F, Huang YX, Han L, Shan B, Gao C, Han J, Dong XP. Human tau protein forms complex with PrP and some GSS- and fCJD-related PrP mutants possess stronger binding activities with tau in vitro. *Mol. Cell. Biochem.* 2008; **310**: 49–55.
23 Lysek DA, Wutrich K. Prion protein interaction with the *C*-terminal SH3 domain of Grb2 studied using NMR and optical spectroscopy. *Biochemistry* 2004; **43**: 10393–10399.
24 Meggio F, Negro A, Sarno S, Ruzzene M, Bertoli A, Sorgato MC, Pinna LA. Bovine prion protein as a modulator of protein kinase CK2. *Biochem. J.* 2000; **352**: 191–196.
25 Surguchev A, Surguchov A. Conformational diseases: looking into the eyes. *Brain Res. Bull.* 2009; **81**: 12–24.

